Cell, Vol. 89, 297–308, April 18, 1997, Copyright ©1997 by Cell Press

MARK, a Novel Family of Protein Kinases That Phosphorylate Microtubule-Associated Proteins and Trigger Microtubule Disruption

Gerard Drewes, Andreas Ebneth, Ute Preuss, Eva-Maria Mandelkow, and Eckhard Mandelkow
Max-Planck-Unit for Structural Molecular Biology
Notkestrasse 85, Gebäude 25B
D-22603 Hamburg
Germany

Summary

MARK phosphorylates the microtubule-associated proteins tau, MAP2, and MAP4 on their microtubule-binding domain, causing their dissociation from microtubules and increased microtubule dynamics. We describe the molecular cloning, distribution, activation mechanism, and overexpression of two MARK proteins from rat that arise from distinct genes. They encode Ser/Thr kinases of 88 and 81 kDa, respectively, and show similarity to the yeast *kin1*$^+$ and C. elegans *par-1* genes that are involved in the establishment of cell polarity. Expression of both isoforms is ubiquitous, and homologous genes are present in humans. Catalytic activity depends on phosphorylation of two residues in subdomain VIII. Overexpression of MARK in cells leads to hyperphosphorylation of MAPs on KXGS motifs and to disruption of the microtubule array, resulting in morphological changes and cell death.

Introduction

The microtubule array plays a central role in a number of cellular processes, such as the regulation of cell shape and cell polarity during differentiation, chromosome partitioning at mitosis, and intracellular transport (reviewed by Drubin and Nelson, 1996; Hyman and Karsenti, 1996). During these processes, microtubules (MTs) undergo rearrangements involving rapid transitions between stable and dynamic states (Sammak and Borisy, 1988). This phenomenon, termed dynamic instability, is a property of the polymer itself (Mitchison and Kirschner, 1984) but is modulated by cellular factors (Belmont and Mitchison, 1996; Walczak et al., 1996). These include the microtubule-associated proteins (MAPs) and filamentous proteins, which stabilize MTs in vitro (Pryer et al., 1992) and in transfected cells (Umeyama et al., 1993). Phosphorylation of MAPs interferes with their MT-stabilizing capacity (Shiina et al., 1992; Trinczek et al., 1995). MAPs isolated from tissue or cells show a varying degree of phosphorylation (Vallee, 1980; Watanabe et al., 1993). In mitotic cells, MAPs exhibit a several-fold higher degree of phosphorylation (Vandre et al., 1991; Preuss et al., 1995), and MT dynamics increase about 20-fold (Saxton et al., 1984). In neurons, MAPs modulate MT organization during morphogenesis and process outgrowth (Caceres and Kosik, 1990; Dinsmore and Solomon, 1991), but even in the axons of mature neurons the dynamic nature of MAP–MT interactions has been shown (Mercken et al., 1995).

We found that phosphorylation of the neuronal MAP tau at a single residue, Ser-262, dramatically reduced MT binding (Biernat et al., 1993). This residue is located in the KXGS sequence within the first of three or four imperfectly repeated motifs that are part of the MT-binding domain. The degree of phosphorylation at KXGS motifs is normally low (Seubert et al., 1995), consistent with a tight association of tau with MTs. It has been shown, however, that phosphorylation of Ser-262 is elevated in tau protein isolated from the neurofibrillary tangles of Alzheimer's disease (Hasegawa et al., 1992), concomitant with a loss of MT binding and aggregation into paired helical filaments (reviewed in Mandelkow et al., 1995).

We partially purified a kinase activity with an apparent molecular mass of 110 kDa (Drewes et al., 1995) that phosphorylates the neuronal MAPs tau and MAP2 and the ubiquitous MAP4 on their homologous KXGS motifs (Illenberger et al., 1996). The kinase caused rapid detachment of all three MAPs from MTs, resulting in high dynamic instability, and was therefore termed MARK (MAP/microtubule affinity-regulating kinase). Here we report the cloning of two cDNAs for MARK encoding protein Ser/Thr kinases that are ubiquitously expressed and show a characteristic domain structure with relationship to genes from yeast and C. elegans. The expression of both isoforms in Chinese hamster ovary (CHO) cells causes the disruption and disappearance of MTs.

Results

Cloning of the Protein Kinase MARK Reveals Two Genes

Recently, we have purified a protein kinase activity that was remarkably efficient in blocking the interactions between MTs and MAPs. We designed a substrate peptide that stems from the main target site on human tau protein around Ser-262. The peptide is specifically phosphorylated by MARK but not by protein kinase A (PKA), which also has a low affinity for the corresponding site in tau (Drewes et al., 1995). Using the peptide to screen for activity of column fractions, 20 μg of pure enzyme was purified. The presence of detergent (0.03% Brij-35) during extraction was essential, suggesting an association with membranous components. In total, the procedure resulted in a 10,000-fold purification (Table 1). These data suggest that the enzyme is a low abundance protein in brain.

Endoprotease Lys-C digestion and peptide sequencing yielded several sequences, two of which were used to design degenerate primers for RT–PCR (Table 2). A 288 bp fragment was amplified from both rat and human brain mRNA, which contained an open reading frame that corresponded to the C-terminal portion of peptide 5, and the lysine residue juxtaposing the 3′ oligonucleotide was consistent with cleavage (data not shown). Screening of a rat brain library with the PCR fragment yielded two types of cDNA derived from distinct genes. One group contained clones of identical sequence with incomplete but overlapping open reading frames. One

Table 1. Purification of MARK from 2 kg of Porcine Brain

Stage	Total Protein (mg)	Total Activity (nmol/min)	Specific Activity (nmol/min/mg)	Recovery (%)	Purification (fold)
Extract	14800	2214	0.15	100	1
Phosphocell.	1500	2212	1.50	100	10
Q-Seph.	216	1512	7.00	68	47
Mono S	55	1072	19.50	48	130
Mono Q	24	655	27.30	29	182
G200	6	414	69.20	19	461
ATP–Seph.	0.05	82	1500	4	10000

clone contained the termination codon, and another contained a putative translational start site (Kozak, 1987). This region of 200 bp showed an 80% G+C content, but no upstream stop codons were found. From these two clones, an open reading frame of 793 amino acids encoding a protein of 88 kDa was derived and termed MARK1. All of the sequenced peptides aligned with the predicted sequence, suggesting that it is the predominant isoform in the isolated enzyme (Figure 1A). Some variations in sequence are noted, mostly in peptides from the regions outside the catalytic domain, which are probably less well conserved among species.

The second group of cDNAs contained one complete and several incomplete clones showing a 72% overall identity with MARK1. The predicted protein, termed MARK2, consists of 722 residues with a molecular mass of 81 kDa and aligns with 7 of the purified peptides. The remaining peptides are unique for MARK1, while none is unique for MARK2. Making use of the rat sequences, we have cloned human *MARK* genes by PCR, yielding sequences with high homology (around 90%) to either rat *MARK1* or *MARK2*, even in untranslated regions (data not shown).

Homologies, Domains, and Structural Predictions

We subdivide the MARK sequences into the following domains: (i) a divergent N-terminal header sequence; (ii) a catalytic domain of 30 kDa containing the common protein kinase motifs; (iii) a ubiquitin-associated (UBA) domain (Hofmann and Bucher, 1996); (iv) an extended spacer region characterized by its highly basic and pronounced hydrophilic character; and (v) a 110-residue C-terminal tail that is basic but more hydrophobic (Figure 1B). Homology between MARK1 and MARK2 is high in the catalytic domain (95%), the UBA domain (85%), and the C-terminal domain (80%) but drops to 50% in the spacer region. There is little secondary structure predicted in the spacer region (PHDsec; Rost and Sander, 1993), but the C-terminus contains two putative amphipathic helices (Segrest et al., 1990).

Phylogenetic analysis of the catalytic domain places MARK in the Snf1/AMPK subfamily of the Ca^{2+}/calmodulin-dependent kinase II (CaMK) group (Hanks and Hunter, 1995) (Figure 1C). Note that although the motif phosphorylated by MARK, i.e., KXGS, is similar to the consensus motifs of PKA, PKC, and CaMK (Kemp and Pearson, 1990), these kinases do not phosphorylate the repeat domain of tau to a comparable extent (Steiner et al., 1990). Pronounced homologies are found with the S. cerevisiae genes *KIN1* and *KIN2* (50%; Levin et al., 1987), the S. pombe gene *kin1* (50%; Levin and Bishop, 1990), and the *par-1* gene of C. elegans (70%; Guo and Kemphues, 1995). Moreover, there is a high degree of homology with two mammalian sequences: EMK, a putative kinase on mouse chromosome 19 (Inglis et al., 1993) that is highly related to MARK2 (97% identity), and human p78 (GenBank no. M80359; unpublished data), which shows 75% homology to MARK1 and 67% to MARK2. In both cases, the encoded proteins have not been characterized. Evidently, the human MARK1/MARK2 homologs and p78 are distinct members of a new protein kinase family.

Tissue Distribution

Northern blots were hybridized with oligonucleotides complementary to sequence regions unique for MARK1 or MARK2. MARK1-specific probes labeled a 4.6 kb mRNA predominantly in rat brain and spleen but also in kidney and skeletal muscle. In other tissues, expression levels were low (Figure 2). The blot was reprobed with MARK2-specific oligonucleotides, which detected a 4.5 kb band in all tissues. The hybridization pattern was similar to MARK1. In adult and fetal human tissues, the rat oligonucleotides detect distinct mRNAs for MARK1 and MARK2, 4.1 and 4.7 kb in size, respectively (Figure 2, right panels). The low intensity of the hybridization signal is presumably due to mismatches between the oligonucleotides and the human mRNAs. The tissue distribution is comparable to that observed in rat tissues. Fetal tissues showed higher expression levels, especially in the kidney. In 7-day mice embryos, we observed no expression of MARK1 and low levels of MARK2, but expression of both isoforms became prominent after 11 days, concomitant with tau expression (data not shown).

Specificity and Regulation of MARK Activity

MARK purified from brain migrates on SDS gels as a fuzzy band with an apparent molecular mass of around 110 kDa (Figure 3A, lane 1), whereas in vitro-translated MARK1 and MARK2 migrated at 100 and 90 kDa, respectively (Figure 3A, lanes 4 and 6), which is slightly higher than predicted, a behavior similar to that reported for the products of the yeast genes *KIN1* and *KIN2* (Donovan et al., 1994). Incubation of brain MARK with phosphatase 2A (PP2A) resulted in a downward shift, both with brain MARK (lane 2) and with proteins translated in vitro (Figure 3A, lanes 5 and 7). In the presence of the phosphatase inhibitor microcystin-LR, higher mobility bands were not observed (Figure 3A, lane 3). Hence, the formation of the fast-migrating band (at 90 kDa) could be due to higher susceptibility of the dephosphorylated protein

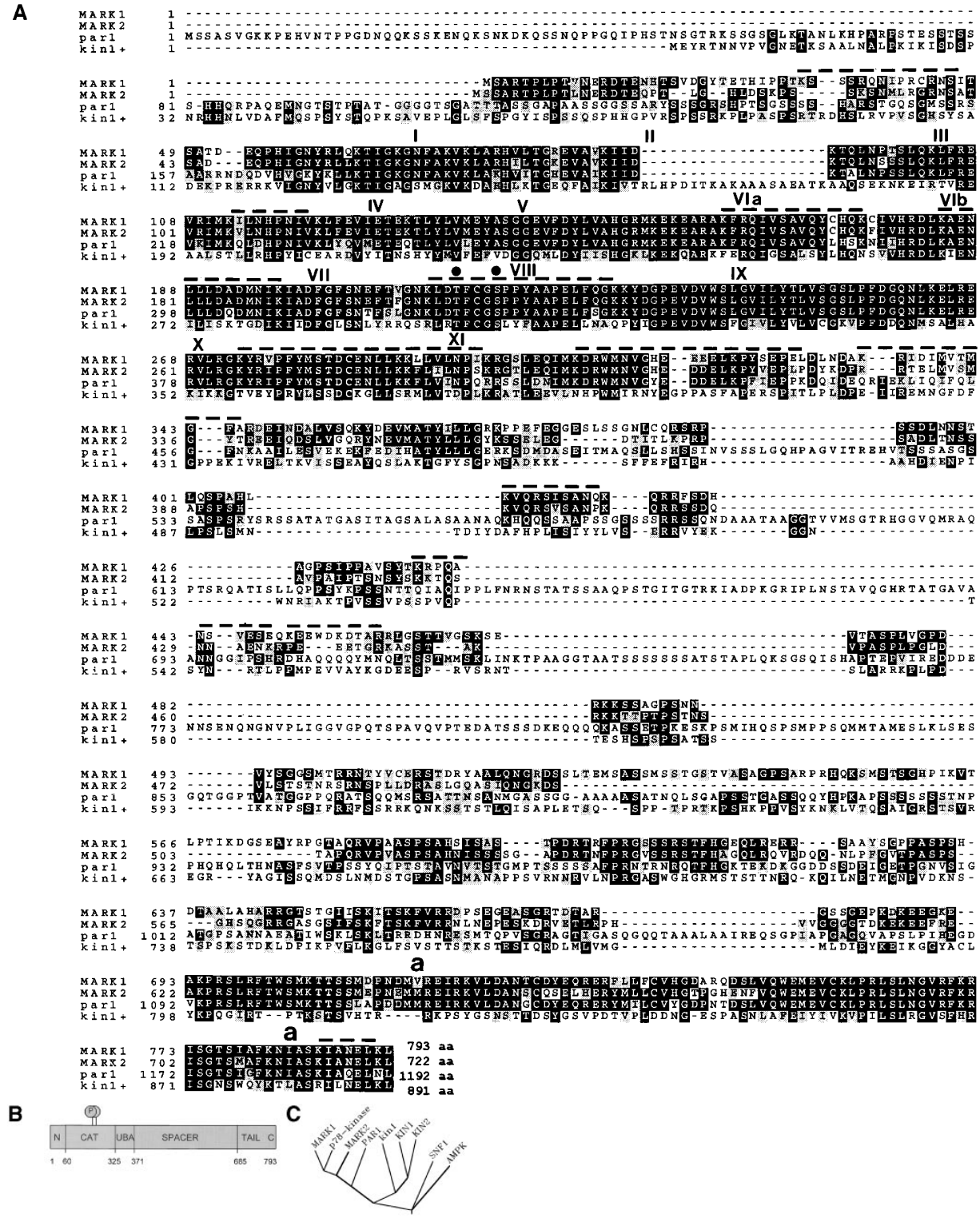

Figure 1. Mammalian Kinases MARK1 and MARK2 and Their Relatives from Nematode and Yeast

(A) Alignment of the predicted amino acid sequences of MARK1 and MARK2 with PAR-1 (C. elegans; Guo and Kemphues 1995) and kin1^{+} (S. pombe; Levin and Bishop, 1990) using CLUSTALW (Thompson et al., 1994). Identical residues are shaded in black, similar residues in grey. The activating phosphorylation sites in subdomain VIII are indicated by dots. Dashed lines above the sequence indicate porcine MARK peptides (Table 2). The catalytic domain is subdivided into subdomains I–XI. Within the tail domain, two predicted amphipathic helices are indicated by "a," N713–L723 and I777–L793.

(B) Diagram of the proposed domain structure of MARK kinases (see text).

(C) Dendrogram of an alignment of the kinases of the SNF1/AMPK subfamily.

Table 2. Peptides Obtained from a Lys-C Digest of Porcine MARK

Peptide	Fraction	Residue No.	MARK Isoform	Peptide Sequence
1	71	34–48	1	(K) XSSRQNIPRCRNNII
				.....S.T
2	88	113–121	1, 2	(K) ILNHPNIVK
3	140	163–176	1, 2	(K) FRQIVSAVQYCHQK
4	47	185–197	1, 2	(K) AENLLLDADMNIK
5	**87**	213–231	1, 2	(K) LDTFCGSPPYAAPELFQGK
6	130	274–286	1, 2	(K) YRIPFYMSTDCENLLK
7	120	291–298	1	(K) LFVLNPIK
				....L.....
8	**33**	308–328	1	(K) DRWMNVGHEEEELKPYAEPEP
				.....S...L
9	140	335–345	1	(K) RIDIMVTMGFL
				.....A
10	93	409–418	1	(K) VQRSISANQK
11	49	440–448	(1, 2)	(K) PQAXNADSE
				R...NSVE..
12	9	451–460	(1)	(K) EEWDRDVARK
				.....K.T..R
13	41	786–793	1, 2	(K) IANELK

The sequences deduced from the rat cDNA for MARK are listed below the peptides where they differ (see Figure 1). Phosphorylated residues in peptide 5 are marked. Peptides 5 and 8 were used for primer construction.

to proteolysis. MARK from brain was also phosphorylated on tyrosine, as detected by immunoblotting (Figure 3A, lanes 8–10).

Dephosphorylation of MARK also affects catalytic activity. We assayed the phosphorylation of peptide TR1 after various incubation times (Figure 3B), revealing that complete inactivation could be achieved with PP2A but not with PTP1B. The presence of ATP during the preincubation led to a small increase in activity, which could be due to autophosphorylation or a copurifying activating factor. The in vitro-translated proteins were also sensitive to PP2A treatment (Figure 3A, lanes 5 and 7). In a number of known protein kinases, a region in subdomain VIII is a target for activating phosphorylation, particularly at a conserved Thr residue (Johnson et al., 1996). We sequenced the corresponding peptide from brain MARK (Table 2, peptide 5). Edman degradation revealed the absence of phenylthiohydantoine (PTH) peaks for Thr and Ser in cycles 3 and 7, instead of which PTH-α-aminodehydrobutyric acid and PTH-dehydroalanine, the products of phospho-Thr and phospho-Ser, appeared (data not shown). The phospho-Thr aligns with the threonines that are essential for activity in a number of protein kinases (Figure 3C). Translation of wild-type and mutant MARKs in reticulocyte lysates showed that activity was lost when each of these residues alone, or both together, were mutated into Ala, and the electrophoretic mobility of the proteins increased. Mutation of the essential Lys residue in subdomain II also resulted in an inactive enzyme that displayed increased mobility, suggesting that the recombinant kinases are activated via autophosphorylation (Figure 3D).

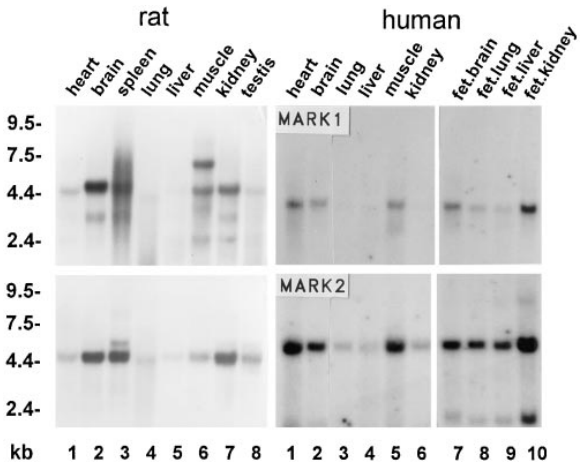

Figure 2. MARK Expression Is Pronounced in Brain, Spleen, Kidney and Muscle

Northern blot analysis of 2 μg of mRNA from rat and human tissues. Size markers in kilobases are indicated. The upper blots show hybridization with MARK1-specific oligonucleotides. Expression is pronounced in brain and spleen, but also in skeletal muscle and kidney. The 6.5 kb band in muscle possibly represents an unrelated mRNA, since it does not hybridize to a cDNA probe for MARK (data not shown). The lower blots show hybridization with MARK2-specific probes. Expression is prominent in brain, spleen, muscle, and kidney. In humans, *MARK*-related mRNAs are prominent in heart and muscle. Relatively high levels of a *MARK2*-related mRNA are found in fetal tissues.

The substrate specificity of the recombinant kinases was investigated by phosphopeptide mapping (Figure 3E). Tryptic maps of tau phosphorylated with in vitro-translated MARK1 or MARK2 were similar to a map obtained from tau phosphorylated with the kinase purified from brain. The pattern shows the typical phosphorylation of KXGS motifs, containing Ser-262, -293, -324, and -356. This result suggests that there is no obvious difference in specificity between MARK1 and MARK2. The fact that the specificity of the recombinant enzymes was comparable to that of the enzyme purified from tissue confirms identity or close relationship of the cloned kinases with the brain enzyme.

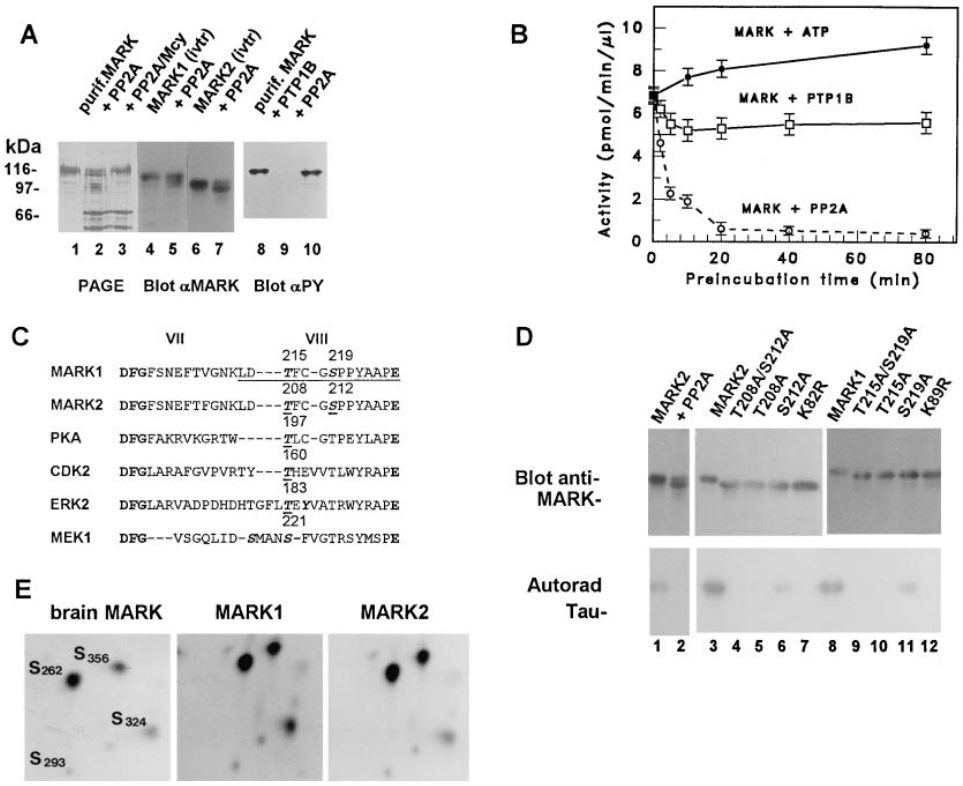

Figure 3. MARK Is Phosphorylated on Ser, Thr, and Tyr Residues, and its Activity Depends on Phosphorylation of Thr-215 and Ser-219

(A) Silver-stained gel showing porcine MARK (lane 1), the same sample after a 20 min incubation with 10 μg/ml PP2A (lane 2), and a control where PP2A was inhibited by microcystin-LR (lane 3). Note the mobility shift concomitant with dephosphorylation. The additional higher mobility bands at 90 kDa are reproducibly formed and could result from an increased proteolytic susceptibility of the dephosphorylated protein. Lanes 4–7 show rat MARK1 and MARK2 translated in reticulocyte lysates, detected by blotting with MARK C-terminal antiserum. Lane 4, MARK1; lane 5, MARK1 dephosphorylated; lane 6, MARK2; lane 7, MARK2 dephosphorylated. Lanes 8–10 show a phosphotyrosine immunoblot. Brain MARK is tyrosine phosphorylated (lane 8), which is sensitive to PTP1B treatment (lane 9) but not to PP2A (lane 10).

(B) Brain MARK activity as dependent on autophosphorylation or dephosphorylation. Purified MARK was incubated with either 100 μM ATP (closed circles), PTP1B (10 μg/ml, open squares), or PP2A (10 μg/ml, open circles). After the indicated time, aliquots were tested for their ability to phosphorylate peptide TR1. Tyr dephosphorylation does not cause a significant decrease in activity, whereas the dephosphorylation of Ser/Thr residues results in complete inactivation.

(C) Alignment of the sequence of a phosphopeptide isolated from porcine brain MARK (Table 2) with the corresponding sequences from several kinases. The phosphorylated Thr-215 in MARK corresponds to the regulatory Thr residue in PKA, CDKs, ERKs, and MEKs.

(D) Point mutations in subdomain VIII affect MARK activity. The activating phosphorylation sites and an essential Lys residue were mutated in MARK1 and MARK2 plasmids as indicated. From these, synthetic RNAs were translated in reticulocyte lysate, and the products immunoprecipitated with anti-HA and anti-C-terminal antibodies. A blot of the samples with the C-terminal antibody is shown. The dephosphorylated sample (lane 2) and the mutants (lanes 4–7 and 9–12) display increased electrophoretic mobility. Catalytic activity was assayed by autoradiography after incubation with [γ-^{32}P]ATP and tau. Only the wild-type enzymes phosphorylate tau efficiently.

(E) Specificity of recombinant MARK. Tryptic digests of the tau samples phosphorylated with MARK1 (lane 8 in [D]) or MARK2 (lane 3 in [D]) were mapped by thin-layer electrophoresis (horizontal) followed by ascending chromatography (vertical). The main spots correspond to the four KXGS motifs in the tau repeats (Drewes et al., 1995). For comparison, a map of tau phosphorylated with porcine brain MARK is shown.

Overexpression of MARK in CHO Cells

By phosphorylating MAPs, MARK catalyzes their detachment from MTs, which results in a decrease in MT stability in vitro (Drewes et al., 1995). We therefore investigated if the kinases would exert a similar effect on the MT array in vivo. CHO cells were transiently transfected with epitope-tagged MARK1 or MARK2 and analyzed by immunofluorescence. A large number of the MARK2-overexpressing cells (Figure 4A) were clearly smaller and more rounded than nontransfected or mock-transfected cells. Besides the small and rounded cells that were obviously no longer viable, we also observed cells that stained positively for the transfected protein but still appeared relatively normal in shape and size. In many of these cells, the disruption of the MT network was striking (Figure 4B). Often, the MTs had almost entirely disappeared. The effect of MARK1 was similar but less severe (Figure 4D). Most transfected cells still showed the typical MT staining pattern, although the network appeared less dense compared with the surrounding nontransfected cells. The transfected cells marked with arrowheads show the early stage of destruction of the MT network. It is interesting to note that we did not observe a destruction of the microfilament network in triple immunofluorescence experiments where labeled phalloidin was used to stain actin (data not shown).

To check if these effects were caused by the phosphorylating activity of the transiently expressed MARK or by other effects of the overexpression, cells were transfected with catalytically inactive mutants. These

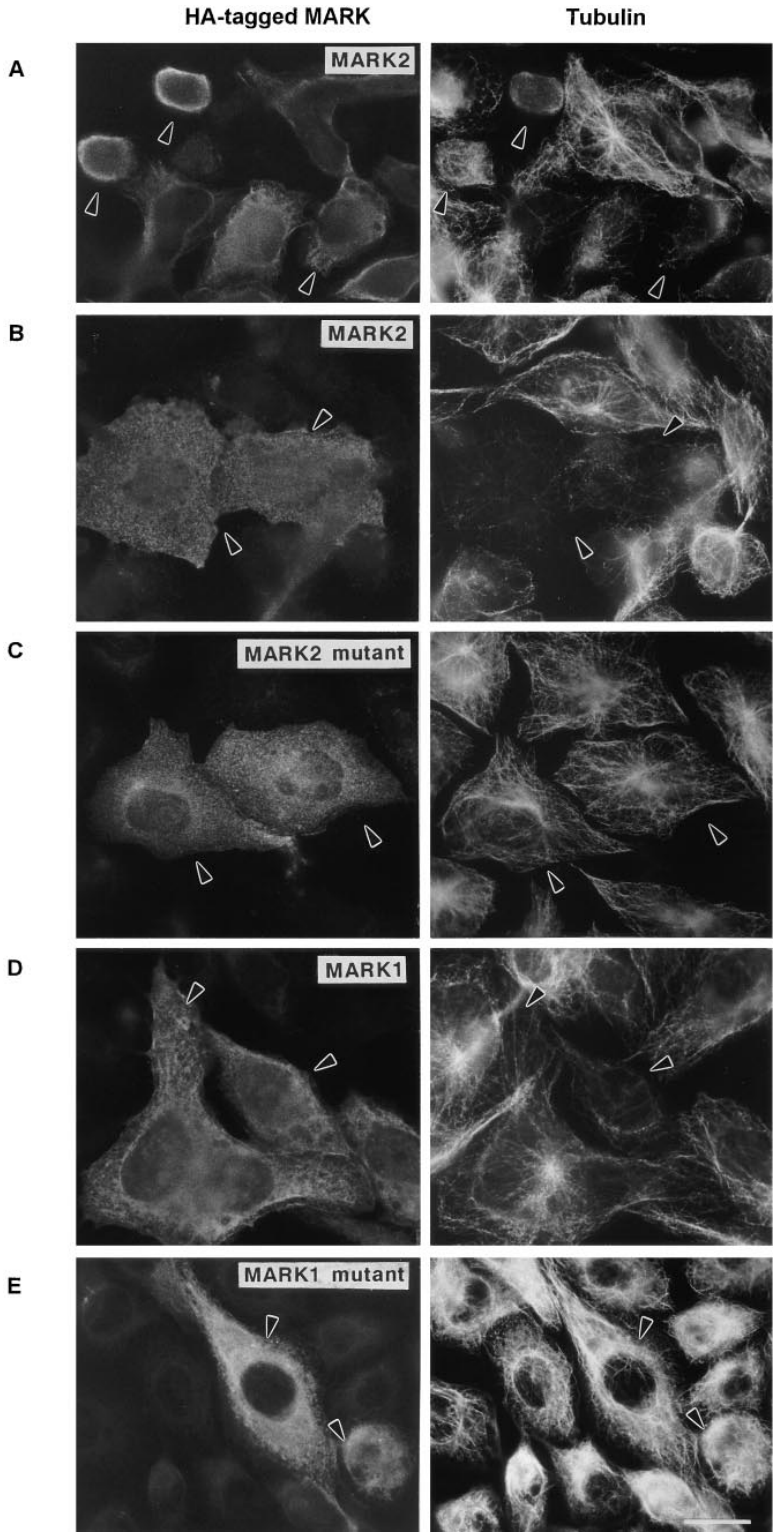

Figure 4. Overexpression of MARK in CHO Cells Causes Breakdown of the Microtubule Array

Double immunofluorescence microscopy of HA-tagged MARKs transfected into CHO cells. After 24 hr, cells were fixed with methanol and stained with anti-HA (left panels) and anti-tubulin (YL1/2) antibodies (right panels). Scale bar = 5 μm.

(A) MARK2-transfected cells tend to be smaller and more rounded in shape, and eventually die.

(B) MARK2-transfected cells showing a dramatic loss of MTs.

(C) Transfection with catalytically inactive MARK2$^{T208A/S212A}$. In contrast to wild-type MARK2, no effect on the MT network is visible.

(D) Cells transfected with MARK1. MT destruction is also observed (arrowheads) but is less pronounced compared to MARK2 overexpression. The staining pattern of the transfected MARK1 is clearly distinct from that of MARK2.

(E) Transfection with inactive MARK1$^{T215A/S219A}$. No effect on the MT network is visible.

cells remained viable, had a normal appearance, and had an intact MT network (Figures 4C and 4E), indicating that the loss of MTs was a consequence of phosphorylation.

The staining of the transfected cells revealed a distinct cytosolic localization for each isoform. MARK2 showed a punctate distribution throughout the cytoplasm, as if it was located to vesicles, whereas the staining of MARK1 suggests its localization to an intracellular network (compare Figure 4B and 4C with 4D and 4E). Note that the inactive mutants show the same staining pattern as the active enzymes.

The effects of MARK overexpression manifest already 8 hr after transfection. The proportion of abnormal cells increases to about 60% of MARK2-positive cells and 40% of MARK1-positive cells after 20 hr (Figure 5A). This can be blocked by the MT-stabilizing drug taxotere (Figure 5B) or by overexpression of MAP2c. Cotransfection of MAP2c$^{S319A/S350A}$, a mutant that binds to MTs irrespective of MARK phosphorylation (Illenberger et al., 1996), was more effective than wild-type MAP2c in counteracting the effects of MARK (Figure 5C). This suggests that the destruction of the MT cytoskeleton directly correlates with the phosphorylation of KXGS motifs.

Since the deleterious effects of the overexpression precluded the recovery of consecutively MARK-expressing cells, we established stable cell lines of MARK2 under control of a doxycyclin-inducible promoter (Gossen et al., 1995). Up to 90% of these cells express MARK, with 5- to 10-fold lower expression levels than in the transient tranfectants, as judged by immunofluorescence. Accordingly, the phenotypic effects are less severe, but still easily discernible, and are counteracted by coexpression of tau (Figure 6, upper left panel) or MAP2c, similar to the experiment of Figure 5. Endogenous MAPs in CHO cells are as yet uncharacterized, and their expression level is low (Barlow et al., 1994); however, the inducible MARK-expressing cells could be transiently cotransfected with tau or MAP2c (Figure 6, left panels). For the detection of site-specific MAP phosphorylation, we used a phosphorylation-dependent antibody that was raised against a phospho-KXGS peptide from the first repeat of tau (12E8) (Seubert et al., 1995). After MARK expression had been induced, the tau-transfected cells brightly stained with the 12E8 antibody (Figure 6, right panels), whereas the staining of endogenous CHO proteins was not observed. In immunoblots of CHO cell extracts, however, a heat-stable 200 kDa band became 12E8 immunoreactive upon induction of MARK2 expression (data not shown).

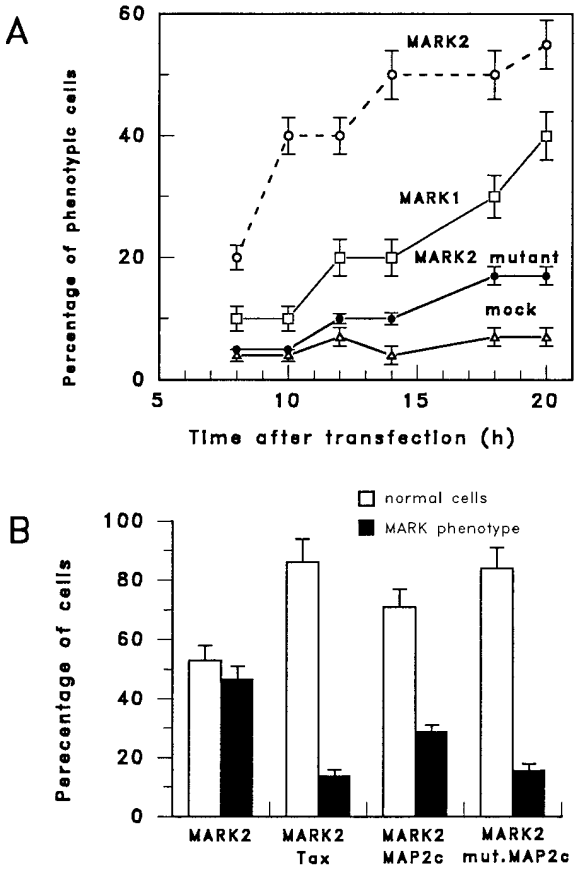

Figure 5. The Phenotypical Effects of MARK Can Be Blocked by Taxotere or Coexpression of MAP2c

(A) Time course of the appearance of morphologically abnormal cells after transfection with MARK2 (open circles), MARK1 (squares) and the inactive MARK2$^{T208A/S212A}$ mutant (closed circles). Triangles show mock-tranfected cells for control. Cells were analyzed by immunofluorescence with anti-HA and anti-tubulin antibodies and regarded as "morphologically abnormal" if they were less than 30% of the average size of untransfected cells, with no distinct MT network visible.

(B) Blocking of MARK2 effects by the microtubule-stabilizing drug taxotere. Cells were counted 18 hr after transfection, as in (A), in parallel experiments with and without 10 μM taxotere.

(C) Partial blocking of MARK2 effects by cotransfection with MAP2c. MAP2$^{cS319A/S350A}$, a mutant in which the two main MARK phosphorylation sites have been eliminated, was more effective in counteracting MARK2 effects than wild-type MAP2c. About 400 cells were counted in each experiment, and mean values of three independent experiments ± SD are shown.

Discussion

This study was originally prompted by several observations relating the phosphorylation of tau protein to Alzheimer's disease. Aggregated tau is the main constituent of the paired helical filaments in the neurofibrillary tangles. The accumulation of these deposits in brain is related to the progression of the dementia (reviewed in Mandelkow et al., 1995). Tau is an MT-associated protein that is thought to stabilize axonal MTs (Binder et al., 1985). However, tau extracted from tangle preparations no longer binds to MTs, and this in turn is presumably related to MT breakdown, interruption of axonal transport, and aggregation into PHFs. Tau isolated from tangles shows characteristically high levels of phosphorylation, particularly at Ser/Thr-Pro motifs, but also at other sites, a prominent one being Ser-262 (Hasegawa et al., 1992). Phosphorylation of this residue turned out to impair strongly tau–MT interactions in vitro (Biernat et al., 1993). This led us to isolate the responsible kinase from brain, now termed MARK (Drewes et al., 1995). Related MAPs such as MAP2 or MAP4 contain similar repeats; they are phosphorylated by MARK at analogous sites with similar effects on MT dynamics (Illenberger et al., 1996).

Two related cDNAs were cloned from a rat brain library, MARK1 (793 residues) and MARK2 (722 residues) (Figure 1). Their sequences may be broadly subdivided into five domains: (i) an N-terminal header, (ii) a catalytic domain, (iii) a UBA domain, (iv) a spacer region, and (v) a C-terminal tail. The header shows little predicted secondary structure and is followed by the catalytic domain, which contains the two activating phosphorylation sites. The adjacent UBA domain argues for a regulation of the enzymes by ubiquitin, possibly by tagging it

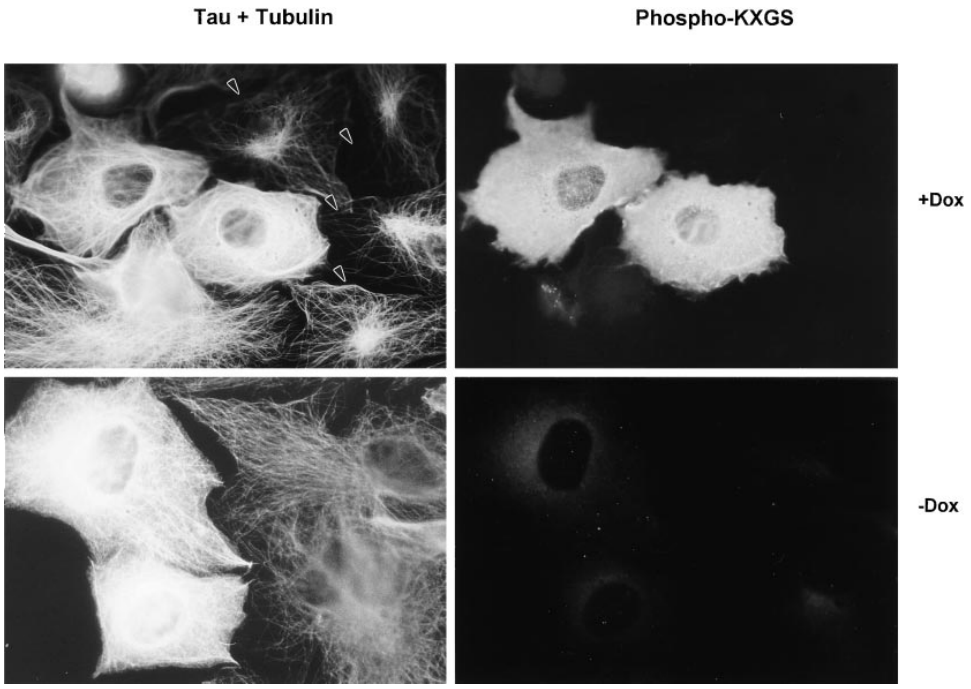

Figure 6. MARK Expression Leads to Hyperphosphorylation of Tau on KXGS Sites

Tau was transiently transfected into CHO cells that stably express MARK2 under control of a doxycyclin-inducible promoter. Cells were fixed with formaldehyde and stained with anti-tau plus anti-tubulin (left panels) and a phospho-tau antibody specific for KXGS-type phosphorylation, 12E8 (right panels). Upper panels show cells in which MARK2 expression is induced, lower panels show the control without induction. The left panels show double staining with tau and tubulin antibodies. Note that, after induction of MARK, the cells that do not express tau (arrowheads) show a weakened microtubule array, compared to the control where no MARK expression had been induced (lower left panel). The bright cells express tau (they are double labeled with tau and tubulin). The microtubule network of the tau-expressing cells remains more intact, presumably because the overexpression of MAPs stabilizes microtubules. The right panels show the phosphorylation of KXGS motifs on tau, as detected by the phosphorylation-dependent antibody 12E8. Phosphorylation of tau at KXGS motifs is observed when MARK expression is induced (upper right panel) but not in the control without doxycyclin induction (lower right panel).

for degradation or membrane recruitment, as reported for the protooncogene c–*cbl* (Wang et al., 1996b). We have indeed observed considerable proteolysis of MARK in extracts from tissue or cells. The spacer region differs from the rest of the protein in its hydrophilic and basic character, and little secondary structure is predicted. Its basicity could point to membrane localization, in agreement with the fact that the kinase activity could only be separated from the particulate fraction by detergent extraction. The spacer domain is most divergent between MARK1 and MARK2 (~50% homology), possibly accounting for the distinct localization in transfected cells (Figure 4). In the C-terminal tail, homology between MARK1 and MARK2 is again high (90%), and two short amphipathic helices are predicted. This points to an identical function of this domain in both enzymes, possibly the interaction with other proteins by coupling to their amphipathic helices (Segrest et al., 1990). It has been reported that the PAR-1 tail domain interacts with myosin II (Guo and Kemphues, 1996). The overall hydrophilic and charges character of the protein might account for the high apparent M_r of 110, compared to its predicted mass of 88 kDa.

The sequence relationship of MARK with kinases from several other organisms might provide a clue to cellular function and, hence, point out directions for future investigations. The protein bearing the highest homology, the human p78, was discovered as a marker that localizes to the apical membrane of epithelial cells but is lost upon carcinogenesis (Parsa, 1988). *KIN1* and *KIN2* (S. cerevisiae) (Levin et al., 1987) show similarity to MARK in their domain organization. Like p78, they localize to the plasma membrane, and their function is unknown (Tibbetts et al., 1994). The related *kin1*$^+$ from S. pombe is required for growth polarity; defective cells grow as spheres (Levin and Bishop, 1990). *par-1*, which shows a still higher homology with MARK, is involved in the establishment of polarity in the early C. elegans embryo (Guo and Kemphues, 1995).

Taken together with the biochemical data, the involvement of MARK-related kinases in the establishment or maintenance of polarity tempts us to hypothesize that MARK might regulate MT dynamics during these events. MTs are key players in the generation of polarity, for instance, in the rotational alignment of the centrosome–nucleus complex in C. elegans and the orientation of the spindle pole body in S. pombe (Chang and Nurse, 1996; White and Strome, 1996), or in neuronal differentiation (Caceres and Kosik, 1990; Dinsmore and Solomon, 1991).

MT-binding proteins containing sequences related to the tau repeats have been found in C. elegans (*ptl-1*; McDermott et al., 1996). The high degree of conservation found only in the repeats argues for a central role of this motif in the function of these proteins. The KVGS motifs in PTL-1 could be targets for phosphorylation by PAR-1. The PAR-1 kinase shows a polar distribution preceding the asymmetric divisions of the early germ cell lineage. This localization is not dependent on its activity, but on other *par* genes and on myosin II. Mutants that are defective in kinase activity perform symmetric first divisions, finally resulting in an amorphous mass of differentiated cells (Guo and Kemphues, 1995, 1996). Failure of PAR-1 to trigger MT dynamics might interfere with the correct placement of the mitotic spindle, which is a determinant of asymmetric division.

MARK1 and MARK2 show a wide tissue distribution, expression being more pronounced in fetal than adult samples. A 100 kDa kinase activity with biochemical characteristics reminiscent of MARK copurifies with MAP2 from chick embryos (Lopez and Sheetz, 1995). It phosphorylated MAP2 and caused the loss of its MT affinity. This activity was not associated with MAP2 purified from adult animals. Since fetal tissues contain higher amounts of proliferating and differentiating cells, a more dynamic regulation of the MT cytoskeleton might be expected, consistent with the observation that fetal MAPs are in a higher phosphorylation state (Watanabe et al., 1993).

One would expect a protein kinase with such potent regulatory function to be strictly regulated itself. We showed that active MARK is a phosphoprotein and that kinase activity was lost after treatment with the Ser/Thr-specific phosphatase 2A. Peptide sequencing data gave us a clue to the activation mechanism. Subdomain VIII of MARK contains phosphorylated Thr-215 and Ser-219, which is analogous to the regulatory loops found in several kinase families, where single or dual phosphorylation is essential for enzyme activity (Johnson et al., 1996). Translation in vitro of MARK point mutants confirmed that Thr-215 and Ser-219 are essential for activity. In the MEKs, ERKs, and CDKs, the phosphorylation is achieved by kinases acting upstream in the respective signaling cascades. Likewise, MARK activity could not be fully restored by autophosphorylation, but we have been able to reactivate dephosphorylated MARK by the addition of crude fractions from brain tissue, which suggests the existence of a distinct activating factor (unpublished data). The phospho-Ser residue is part of a Ser–Pro motif and hence might be a target of upstream proline-directed kinases. Brain MARK contains phosphotyrosine, but here the dephosphorylation has no severe effect on the enzymatic activity. However, other functions, e.g. in protein–protein interactions, are not excluded.

Overexpression of both MARK isoforms in CHO cells revealed dramatic effects. Cells grew smaller and rounded, their MT array became disorganized or disappeared, and cells eventually died. The effect is dependent on the enzymatic activity of the kinases; expression of inactive mutants had no effect. The effect of MARK2 was more pronounced than that of MARK1. This is probably due to differences in regulation or localization, since the catalytic domains of both kinases are very similar and, in the case of tau protein, have identical substrate specificities in vitro. If MARK expression is induced in cells transfected with tau, the cells stain with antibody 12E8, which detects phosphorylated KXGS motifs in MAPs. The deleterious effects of MARK overexpression could be blocked by the presence of the MT-stabilizing drug taxotere, suggesting that the changes in morphology resulting from MARK expression are indeed mediated by MT destabilization. Coexpression of tau and, more pronounced, MAP2c also counteracted the phenotype induced by MARK. This protective effect was enhanced if a mutant MAP2c was coexpressed in which the main MARK target sites had been eliminated and which thus binds to MTs irrespective of phosphorylation. These data strengthen the hypothesis that MT destabilization is mediated by MARK phosphorylation of MAPs.

The transfection experiments raise a few questions about the current view of how the MT cytoskeleton might be regulated. MAPs appear to be essential for certain aspects of the cell cycle or differentiation involving MTs (e.g., tau and MAP2 in neuronal differentiation [Caceres and Kosik, 1990; Dinsmore and Solomon, 1991]; MAP4 in myogenesis [Mangan and Olmsted, 1996]). Other work suggests that removal of MAPs has no major consequence. For example, removal of MAP4 from MTs in fibroblasts resulted in no obvious effects (Wang et al., 1996a), and mice lacking a functional *tau* gene did not show a severe phenotype (Harada et al., 1994). These results, however, might be explained by a functional redundancy between the MAPs; i.e., cellular effects might become visible only when several MAPs are impaired simultaneously. Cases of this kind are documented for actin-binding proteins in Dictyostelium discoideum (Witke et al., 1992). The observed disruption of the MT cytoskeleton could be a consequence of the reduced stability of the MTs lacking MAPs. Such MAP-deficient MTs could be prone to disruption, for example, by catastrophe factors (Belmont and Mitchison, 1996; Walczak et al., 1996).

In summary, MARKs phosphorylate MAPs and have the potential to disrupt the MT network. Active MARKs are phosphorylated, probably by upstream factors. This could provide a mechanism by which extracellular signals control the stability of the cytoskeleton. MARK-related proteins in other organisms are involved in the development of cell polarity. In Alzheimer's disease, the neuronal polarity is lost, and axonal tau protein accumulates in the somatodendritic compartment. Hence, one might speculate that a defect in MARK function could be a common link.

Experimental Procedures

Purification of MARK

Porcine brains (2 kg) were homogenized in 2 l of buffer A (100 mM Tris–HCl [pH 8.6], 2 mM EDTA, 100 mM NaF, 1 mM PMSF, 2 mM benzamidine, 1 mM Na_3VO_4, 1 mM DTT, 0.06% Brij-35), centrifuged at 100,000 × g for 1 hr, and the extract was loaded onto a Whatman P11 column (10 × 5 cm) in buffer B (50 mM MES [pH 6.8], 2 mM EGTA, 50 mM NaF, 1 mM PMSF, 1 mM benzamidine, 1 mM Na_3VO_4, 1 mM DTT, 0.03% Brij-35). The column was washed with 1 l of buffer B plus 150 mM NaCl and eluted with a 750 ml gradient (0.15–1 M

NaCl) at 15 ml/min. Fractions were assayed by phosphorylation of a synthetic peptide, TR1 (NVKSKIGSTENLK). Pools were dialyzed against buffer A, loaded onto Q-Sepharose (Pharmacia; 80 × 16 mm), and eluted with a gradient from 0–0.5 M NaCl (flow rate = 5 ml/min, 7 ml fractions). The active pool (40 ml) was desalted on Sephadex G25 and loaded onto a Mono S HR10/10 column (Pharmacia; flow rate = 4 ml/min, 7 ml fractions). Active fractions (40 ml) were concentrated on a Mono Q HR 5/5 column and gel filtered (Pharmacia Superdex 200; 300 × 16 mm) in buffer A (adjusted to pH 7.8 plus 150 mM NaCl, flow rate = 0.1 ml/min, 2 ml fractions). After gel filtration in buffer C (40 mM β-glycerophosphate containing 10 mM $MgCl_2$, 2 mM EGTA, 1 mM benzamidine, 0.2 mM DTT), active pools were loaded at 0.05 ml/min onto a 1 ml column of γ-phosphate-linked ATP–Sepharose (UBI). The enzyme was eluted with 5 mM MgATP, dialyzed against buffer A containing 50% (v/v) glycerol, and stored at −20°C. Twenty micrograms of purified MARK was incubated with 6 M urea and 2 mM DTT for 2 hr at 30°C and reacted with 5 mM 4-vinylpyridine for 4 hr. After addition of 10 mM DTT, the sample was gel filtered into 20 mM NH_4HCO_3 and digested with 2 μg of endoprotease Lys-C (Promega). Peptides were separated on a Vydac 218TP52 column with a 16 ml gradient of 0%–60% acetonitrile in 10 mM ammoniumacetate at 100 μl/min, further purified on a Pharmacia μRPCC2/C18 column using a 10 ml gradient of 10% (v/v) acetonitrile in 0.075% TFA to 66% acetonitril in 0.05% TFA at 80 μl/min, and sequenced on a 476A sequencer (ABI). Phosphoserines and -threonines were identified as DTT adducts of PTH-dehydroalanine or α-aminodehydrobutyric acid (Meyer et al., 1993).

cDNA Cloning

The sequences obtained from fractions 87 and 33 were used for the design of degenerate primers GA[CT]ACNTT[CT]TG[CT]GGN [AT][CG]NCC and [CT]TC[AG]TC[AG]TC[CT]TC[AG]TGNCCNAC[AG] TTCATCCA, which were used in an RT–PCR with 0.1 μg rat brain or human brain mRNA (Clontech). cDNA synthesis by AMV reverse transcriptase (primed with oligo[dT] at 42°C for 1 hr) was followed by amplification by Pyrococcus furiosus DNA-polymerase (Stratagene) (30 cycles of 94°C, 1 s, 59°C, 30 s, and 71°C, 60 s). The products were reamplified in a nested PCR with GCNCCNGA[AG][CT]TNTT [CT]CA[AG]GG designed from the C-terminal portion of peptide 87. The amplified fragment was cloned and sequenced. Labeled probes were generated by PCR using [α-^{32}P]dATP and used to screen 10^6 clones of a rat brain cDNA library in λZAPII (Stratagene). Filters were hybridized in 5× SSPE (0.4 M NaH_2PO_4 [pH 7.4], 0.75 M NaCl, 5 mM EDTA), 100 μg/ml salmon sperm DNA, 5× Denhardt's, 1% (w/v) SDS, and 50% (v/v) formamide at 42°C for 16 hr and washed in 0.2× SSPE, 0.1% SDS at 60°C for 3 × 30 min. Six positive plaques (pBlK1–pBlK6) were identified by autoradiography and further purified by the same procedure. From these, pBluescript plasmids were rescued and sequenced on both strands. For the missing 5′-end of clone pBlK1, the screening was repeated using a 350 bp probe generated by PCR from the 5′-end of the incomplete clone. An overlapping clone (pBlK7) was isolated and fused to pBlK1, yielding pBlK17.

Northern Blotting

Northern blots were performed using 2 μg of poly(A)$^+$ RNA isolated from different tissues, fractionated by denaturing agarose gel electrophoresis, and transferred to nylon membranes (Clontech). Equal loading was ensured by hybridization with an actin probe. cDNA probes for MARK were generated by random primer labeling or PCR. Oligonucleotide probes (45-mers) for MARK1 and MARK2 were designed in divergent regions (amino acids 28–42 and 667–681 in MARK1 and amino acids 19–33 and 592–604 in MARK2). The probes (1–3 pmol) were labeled to 10^7 cpm/pmol by T4 polynucleotide kinase and/or terminal transferase (Boehringer) and hybridized in 5× SSPE, 2× Denhardt's, 100 μg/ml salmon sperm DNA, and 0.5% SDS at 42°C. Washes were conducted in 0.5× SSPE, 1% SDS.

Plasmids

The coding regions of pBlK17 (MARK1) and pBlK2 (MARK2) were subcloned into pEUHATag, a modified form of pRc/CMV (Invitrogen), using synthetic linkers or PCR with primers containing appropriate restriction sites. For doxycyclin-inducible expression, we constructed plasmid pIndMARKII by inserting the coding region of pBlK2 into pUHD10–3 (Gossen et al., 1995). pUHD172–1neo was a gift of Dr. H. Bujard, ZMBH Heidelberg (Gossen et al., 1995). All MARK plasmids were 5′-tagged by insertion of a sequence derived from influenza haemagglutinin (HA), CATATGGGATCCTACCCTTAC GACGTCCCTGACTACGCGTCCGATA. Site-directed mutagenesis was performed using the QuickChange kit (Stratagene). Human cDNAs for tau40 and MAP2c were gifts of Drs. M. Goedert (MRC Cambridge, UK) and C. Garner (University of Alabama, Birmingham, AL), respectively, and were inserted into pEUHATag.

Antibodies

The following antibodies were used: Mouse monoclonals anti-HA (12CA5; Boehringer), anti-TauS262P (12E8; a gift from Dr. D. Schenk, Athena Neuroscience), anti-P-Tyr (4G10; UBI), and anti-tubulin (DM1A; Sigma); rat anti-tubulin (YL1/2; Sera-lab); and rabbit polyclonal anti-tau (Dako). Secondary antibodies were fluorescein-conjugated goat anti-mouse and rhodamine-conjugated goat anti-rat and anti-rabbit (Dianova). Rabbit antisera were raised against MARK N- and C-terminal peptides MSSARTPLPTLNERD and KNIASKIANELKL.

In Vitro Translation

Linearized plasmids were transcribed by T7 RNA polymerase and translated in reticulocyte lysate (Promega). Products were analyzed by blotting with MARK C-terminal antiserum. One-hundred-microliter samples were gel filtered on a Pharmacia Superose 12–2.1/30 column in 40 mM HEPES (pH 7.2), 5 mM $MgCl_2$, 2 mM EGTA; 0.1 mM DTT, 0.2 mM PMSF, 0.03% Brij-35, and the fraction eluting at the position of phosphorylase B (97 kDa, used for calibration) was subjected to immunoprecipitation with anti-HA antibody prebound to protein A/G-agarose (Dianova). Peptide TR1 (50 μM) or htau40 (3 μM) and [γ-^{32}P]ATP (10 μM, 500 Ci/mmol, New England Nuclear) were incubated with the immunoprecipitates for 30 min at 37°C. Phosphopeptide quantitation and mapping was performed as described (Drewes et al., 1995).

Dephosphorylation Assay

Purified brain MARK (1 mU, transfers 1 nmol P_i/min to MAP2c at 37°C) was incubated with 0.5 μg PP2A or PTP1B (a gift of Dr. N. Tonks, Cold Spring Harbor Laboratory, NY) in 50 mM Tris–HCl (pH 7.4), 0.1 mM DTT, 0.1 mM PMSF, 5% (v/v) glycerol, final volume 50 μl, at 37°C. The reactions were terminated by the addition of microcystin-LR (1 μM, Biomol) or Na_3VO_4 (1 mM).

Cell Culture

CHO cells were grown in HAM's F12 medium/10% FCS/5% CO_2 at 37°C, seeded at 70% confluency in 24-well plates on coverslips, and transfected with 1 μg of DNA using 2 μl lipofectamine (GIBCO) or DOTAP (Boehringer Mannheim). Stable transfectants of pUHD172–1neo were selected in the presence of 800 μg/ml geneticin (CHO172–1). For inducible expression, pIndMARK2 was cotransfected with pBabePuro into CHO172–1 cells, and stable transfectants recloned in the presence of 2 μg/ml puromycin. Expression was induced with 1 μg/ml doxycyclin for 1–2 days. Immunofluorescence analysis was performed 8–24 hr after transfection. Cells were washed in 80 mM Pipes, 1mM $MgCl_2$, 1 mM EGTA, 4% (w/v) polyethylene glycol (pH 6.9), fixed with methanol at −20°C for 5 min or paraformaldehyde for 30 min at 37°C, permeabilized with 0.2% Triton X-100 in PBS, treated with 5% nonfat dry milk in PBS for 1 hr, and incubated with primary antibody for 1 hr at 37°C and with secondary antibody at 1:300 dilution for 30 min. All reagents were from Sigma, and taxotere was from Rhone-Poulenc Rorer (Vitry, France). Microscopy was performed with a Zeiss Axioplan using filters optimized for double-label experiments and a 63× objective.

Acknowledgments

Correspondence should be addressed to G. D. (e-mail: drewes@mpasmb.desy.de). Help during the initial stage of this work from Drs. F. Döring and J. Biernat (Hamburg) with cloning and mutagenesis and from Dr. H. E. Meyer (Ruhr-University Bochum) with peptide sequencing is gratefully acknowledged. We thank U. Böning, A.

Miegel, and I. Thielke for excellent technical assistance, and T. Timm for help with sequencing. G. D. received part-time support from the Deutsche Forschungsgemeinschaft (GRK-255/1–96 Neuronale Signaltransduktion und deren pathologische Störungen).

Received July 25, 1996; revised March 7, 1997.

References

Barlow, S., Gonzalez-Garay, M.L., West, R., Olmsted, J.B., and Cabral, F. (1994). Stable expression of heterologous microtubule-associated proteins (MAPs) in Chinese hamster ovary cells: evidence for differing roles of MAPs in microtubule organization. J. Cell Biol. *126*, 1017–1029.

Belmont, L.D., and Mitchison, T.J. (1996). Identification of a protein that interacts with tubulin dimers and increases the catastrophe rate of microtubules. Cell *84*, 623–631.

Biernat, J., Gustke, N., Drewes, G., Mandelkow, E.-M., and Mandelkow, E. (1993). Phosphorylation of Ser^{262} strongly reduces the binding of tau protein to microtubules: distinction between PHF-like immunoreactivity and microtubule binding. Neuron *11*, 153–163.

Binder, L.I., Frankfurter, A., and Rebhun, L.I. (1985). The distribution of tau in the mammalian central nervous system. J. Cell Biol. *101*, 1371–1378.

Caceres, A., and Kosik, K.S. (1990). Inhibition of neurite polarity by tau antisense oligonucleotides in primary cerebellar neurons. Nature *343*, 461–463.

Chang, F., and Nurse, P. (1996). How fission yeast fission in the middle. Cell *84*, 191–194.

Dinsmore, J.H., and Solomon, F. (1991). Inhibition of MAP2 expression affects both morphological and cell division phenotypes of neuronal differentiation. Cell *64*, 817–826.

Donovan, M., Romano, P., Tibbetts, M., and Hammond, C.I. (1994). Characterization of the *KIN2* gene product in Saccharomyces cerevisiae and comparison between the kinase activities of p145KIN1, and p145KIN2. Yeast *10*, 113–124.

Drewes, G., Trinczek, B., Illenberger, S., Biernat, J., Schmitt-Ulms, G., Meyer, H.E., Mandelkow, E.M., and Mandelkow, E. (1995). p110mark: A novel protein kinase that regulates tau–microtubule interactions and dynamic instability by phosphorylation at the Alzheimer-specific site Serine 262. J. Biol. Chem. *270*, 7679–7688.

Drubin, D.G., and Nelson, W.J. (1996). Origins of cell polarity. Cell *84*, 335–344.

Gossen, M., Freundlieb, S., Bender, G., Müller, G., Hillen, W., and Bujard, H. (1995). Transcriptional activation by tetracyclines in mammalian cells. Science *268*, 1766–1769.

Guo, S., and Kemphues, K.J. (1995). *par-1*, a gene required for establishing polarity in C. elegans embryos, encodes a putative Ser/Thr kinase that is asymmetrically distributed. Cell *81*, 611–620.

Guo, S., and Kemphues, K.J. (1996). A non-muscle myosin required for embryonic polarity in Caenorhabditis elegans. Nature *382*, 455–458.

Hanks, S.K., and Hunter, T. (1995). Protein kinases 6. The eukaryotic protein kinase superfamily: kinase catalytic domain structure and classification. FASEB J. *9*, 576–596.

Harada, A., Oguchi, K., Okabe, S., Kuno, J., Terada, S., Ohshima, T., Sato-Yoshitake, R., Takei, Y., Noda, T., and Hirokawa, N. (1994). Altered microtubule organization in small-calibre axons of mice lacking tau protein. Nature *369*, 488–491.

Hasegawa, M., Morishima-Kawashima, M., Takio, K., Suzuki, M., Titani, K., and Ihara, Y. (1992). Protein sequence and mass spectrometric analysis of tau in the Alzheimer's disease brain. J. Biol. Chem. *267*, 17047–17054.

Hofmann, K., and Bucher, P. (1996). The UBA-domain: a sequence motif found in multiple enzyme classes of the ubiquitination pathway. Trends Biochem. Sci. *21*, 172–173.

Hyman, A.A., and Karsenti, E. (1996). Morphogenetic properties of microtubules and mitotic spindle assembly. Cell *84*, 401–410.

Illenberger, S., Drewes, G., Trinczek, B., Biernat, J., Meyer, H.E., Olmstedt, J.B., Mandelkow, E.M., and Mandelkow, E. (1996). Phosphorylation of microtubule-associated proteins MAP2 and MAP4 by the protein kinase p110mark. J. Biol. Chem. *271*, 10834–10843.

Inglis, J.D., Lee, M., and Hill, R.E. (1993). Emk, a protein kinase with homologs in yeast maps to mouse chromosome 19. Mammalian Genome *4*, 401–403.

Johnson, L.N., Noble, M.E.M., and Owen, D.J. (1996). Active and inactive protein kinases: structural basis for regulation. Cell *85*, 149–158.

Kemp, B.E., and Pearson, R.B. (1990). Protein kinase recognition sequence motifs. Trends Biochem. Sci. *15*, 342–346.

Kozak, M. (1987). An analysis of 5′-noncoding sequences from 699 vertebrate messenger RNAs. Nucleic Acids Res. *15*, 8125–8148.

Levin, D.E., Hammond, C.I., Ralston, R.O., and Bishop, M.J. (1987). Two yeast genes that encode unusual protein kinases. Proc. Natl. Acad. Sci. USA *84*, 6035–6039.

Levin, D.E., and Bishop, M.J. (1990). A putative protein kinase gene ($kin1^{+}$) is important for growth polarity in Schizosaccharomyces pombe. Proc. Natl. Acad. Sci. USA *87*, 8272–8276.

Lopez, L.A., and Sheetz, M.P. (1995). A microtubule-associated protein (MAP2) kinase restores microtubule motility in embryonic brain. J. Biol. Chem. *270*, 12511–12517.

Mandelkow, E.-M., Biernat, J., Drewes, G., Gustke, N., Trinczek, B., and Mandelkow, E. (1995). Tau domains, phosphorylation, and interactions with microtubules. Neurobiol. Aging *16*, 355–362.

Mangan, M.E., and Olmsted, J.B. (1996). A muscle-specific variant of microtubule-associated protein 4 (MAP4) is required in myogenesis. Development *122*, 771–781.

McDermott, J.B., Aamodt, S., and Aamodt, E. (1996). *ptl-1*, a *Caenorhabditis elegans* gene whose products are homologous to the τ microtubule-associated proteins. Biochemistry *35*, 9415–9423.

Mercken, M., Fischer, I., Kosik, K.S., and Nixon, R.A. (1995). Distinct axonal-transport rates for tau, tubulin, and other microtubule-associated proteins—evidence for dynamic interactions of tau with microtubules in vivo. J. Neurosci. *15*, 8259–8267.

Meyer, H.E., Eisermann, B., Heber, M., Hoffmann-Posorske, E., Korte, H., Weigt, C., Wegner, A., Hutton, T., Donella-Deana, A., and Perich, J.W. (1993). Strategies for nonradioactive methods in the localization of phosphorylated amino acids in proteins. FASEB J. *7*, 776–782.

Mitchison, T., and Kirschner, M. (1984). Dynamic instability of microtubule growth. Nature *312*, 237–242.

Parsa, I. (1988). Loss of a M_r 78,000 marker in chemically induced transplantable carcinomas and primary carcinoma of human pancreas. Cancer Res. *48*, 2265–2272.

Preuss, U., Döring, F., Illenberger, S., and Mandelkow, E.M. (1995). Cell cycle dependent phosphorylation and microtubule binding of tau protein stably transfected into chinese hamster ovary cells. Mol. Biol. Cell *6*, 1397–1410.

Pryer, N.K., Walker, R.A., Skeen, V.P., Bourns, B.D., Soboeiro, M.F., and Salmon, E.D. (1992). Brain microtubule-associated proteins modulate microtubule dynamic instability in vitro. Real-time observations using video microscopy. J. Cell Sci. *103*, 965–976.

Rost, B., and Sander, C. (1993). Prediction of protein secondary structure at better than 70% accuracy. J. Mol. Biol. *232*, 584–599.

Sammak, P.J., and Borisy, G.G. (1988). Direct observation of microtubule dynamics in living cells. Nature *332*, 724–726.

Saxton, W.M., Stemple, S.L., Leslie, R.J., Salmon, E.D., Zavortink, M., and McIntosh, J.R. (1984). Tubulin dynamics in cultured mammalian cells. J. Cell Biol. *99*, 2175–2186.

Segrest, J.P., De Loof, H., Dohlman, J.H., Brouillette, C.G., and Anantharamaiah, G.M. (1990). Amphipathic helix motif: classes and properties. Proteins *8*, 103–117.

Seubert, P., Mawal-Dewan, M., Barbour, R., Jakes, R., Goedert, M., Johnson, G.V.W., Litersky, J.M., Schenk, D., Lieberburg, I., Trojanowski, J.Q., and Lee, V.M.Y. (1995). Detection of phosphorylated Ser-262 in fetal tau, adult tau, and paired helical filament tau. J. Biol. Chem. *270*, 18917–18922.

Shiina, N., Moriguchi, T., Ohta, K., Gotoh, Y., and Nishida, E. (1992). Regulation of a major microtubule-associated protein by MPF and MAP kinase. EMBO J. *11*, 3977–3984.

Steiner, B., Mandelkow, E.-M., Biernat, J., Gustke, N., Meyer, H.E., Schmidt, B., Mieskes, G., Söling, H.D., Drechsel, D., Kirschner, M.W., Goedert, M., and Mandelkow, E. (1990). Phosphorylation of microtubule-associated protein tau: identification of the site for Ca^{++}/calmodulin dependent kinase and relationship with tau phosphorylation in Alzheimer tangles. EMBO J. *9*, 3539–3544.

Thompson, J.D., Higgins, D.G., and Gibson, T.J. (1994). CLUSTALW: improving the sensitivity of progressive multiple sequence alignment through sequence weighting, positions-specific gap penalties and weight matrix choice. Nucleic Acids Res. *22*, 4673–4680.

Tibbetts, M., Donovan, M., Roe, S., Stiltner, A.M., and Hammond, C.I. (1994). KIN1 and KIN2 protein kinases localize to the cytoplasmic face of the yeast plasma membrane. Exp. Cell Res. *213*, 93–99.

Trinczek, B., Biernat, J., Baumann, K., Mandelkow, E.M., and Mandelkow, E. (1995). Domains of tau-protein, differential phosphorylation, and dynamic instability of microtubules. Mol. Biol. Cell *6*, 1887–1902.

Umeyama, T., Okabe, S., Kanai, Y., and Hirokawa, N. (1993). Dynamics of microtubules bundled by microtubule associated protein-2c. J. Cell Biol. *120*, 451–465.

Vallee, R.B. (1980). Structure and phosphorylation of microtubule-associated protein 2 (MAP2). Proc. Natl. Acad. Sci. USA *77*, 3206–3210.

Vandre, D.D., Centonze, V.E., Peloquin, J., Tombes, R.M., and Borisy, G.G. (1991). Proteins of the mammalian mitotic spindle: phosphorylation/dephosphorylation of MAP-4 during mitosis. J. Cell Sci. *98*, 577–588.

Walczak, C.E., Mitchison, T.J., and Desai, A. (1996). XKCM1: a Xenopus kinesin-related protein that regulates microtubule dynamics during mitotic spindle assembly. Cell *84*, 37–47.

Wang, X.M., Peloquin, J.G., Zhai, Y., Bulinski, J.C., and Borisy G.G. (1996a). Removal of MAP4 from microtubules in vivo produces no observable phenotype at the cellular level. J. Cell Biol. *132*, 345–357.

Wang, Y., Yeung, Y.G., Langdon, W.Y., and Stanley, E.R. (1996b). c-Cbl is transiently tyrosine-phosphorylated, ubiquitinated, and membrane-targeted following CSF-1 stimulation of macrophages. J. Biol. Chem. *271*, 17–20.

Watanabe, A., Hasegawa, M., Suzuki, M., Takio, K., Morishima-Kawashima, M., Titani, K., Arai, T., Kosik, K.S., and Ihara, Y. (1993). In vivo phosphorylation sites in fetal and adult rat tau. J. Biol. Chem. *268*, 25712–25717.

White J., and Strome, S. (1996). Cleavage plane specification in C. elegans: how to divide the spoils. Cell *84*, 195–198.

Witke, W., Schleicher, M., and Noegel, A.A. (1992). Redundancy in the microfilament system: abnormal development of Dictyostelium cells lacking two F-actin cross-linking proteins. Cell *68*, 53–62.

GenBank Accession Numbers

The GenBank accession numbers for the MARK1 and MARK2 sequences are Z83868 and Z83869, respectively.